PUBLISHED VERSION

Carly Whittaker, Christopher A.G. Kalnins, David Ottaway, Nigel A. Spooner and Heike Ebendorff-Heidepriem

Transmission loss measurements of plastic scintillating optical fibres

Optical Materials Express, 2019; 9(1):1-12

DOI: http://dx.doi.org/10.1364/OME.9.000001

© 2018 Optical Society of America under the terms of the OSA Open Access Publishing Agreement. Users may use, reuse, and build upon the article, or use the article for text or data mining, so long as such uses are for non-commercial purposes and appropriate attribution is maintained. All other rights are reserved.

PERMISSIONS

https://www.osapublishing.org/submit/review/copyright_permissions.cfm#posting

Author and End-User Reuse Policy

OSA's policies afford authors, their employers, and third parties the right to reuse the author's Accepted Manuscript (AM) or the final publisher Version of Record (VoR) of the article as outlined below:

Reuse purpose	Article version that can be used under:		
	Copyright Transfer	Open Access Publishing Agreement	CC BY License
Posting by authors on an open institutional repository or funder repository	AM after 12 month embargo	VoR	VoR

Attribution

Open access articles

If an author or third party chooses to post an open access article published under OSA's OAPA on his or her own website, in a repository, on the arXiv site, or anywhere else, the following message should be displayed at some prominent place near the article and include a working hyperlink to the online abstract in the OSA Journal:

> © XXXX [year] Optical Society of America]. Users may use, reuse, and build upon the article, or use the article for text or data mining, so long as such uses are for non-commercial purposes and appropriate attribution is maintained. All other rights are reserved.

When adapting or otherwise creating a derivative version of an article published under OSAs OAPA, users must maintain attribution to the author(s) and the published article's title, journal citation, and DOI. Users should also indicate if changes were made and avoid any implication that the author or OSA endorses the use.

29 June 2021

http://hdl.handle.net/2440/117921

Research Article | Vol. 9, No. 1 | 1 Jan 2019 | OPTICAL MATERIALS EXPRESS 1
Optical Materials EXPRESS

Transmission loss measurements of plastic scintillating optical fibres

CARLY WHITTAKER,[1,*] CHRISTOPHER A. G. KALNINS,[1] DAVID OTTAWAY,[1,2] NIGEL A. SPOONER,[1,2,3] AND HEIKE EBENDORFF-HEIDEPRIEM[1,2]

[1]*Institute for Photonics and Advanced Sensing (IPAS) and the School of Physical Sciences, The University of Adelaide, Adelaide, South Australia 5005, Australia*
[2]*ARC Research Hub for Australian Copper-Uranium, The University of Adelaide, Adelaide, South Australia 5005, Australia*
[3]*DST Group, PO Box 1500, Edinburgh, SA 5111, Australia*
[*]*carly.whittaker.1@ulaval.ca*

Abstract: The wavelength dependent attenuation spectra of a range of commercially available and in-house fabricated scintillating polymer optical fibres have been measured using cut-back and side induced fluorescence techniques. The fibre transmission loss was found to be dependent on the scintillator formulation, core size and cladding, the effects of which are discussed in relation to various intrinsic and extrinsic loss sources.

© 2018 Optical Society of America under the terms of the OSA Open Access Publishing Agreement

1. Introduction

Plastic scintillating fibres are widely used in radiation dosimetry applications because of their compact form, high sensitivity, fast response and immunity to electro-magnetic interference. Their real-time, remote readout capability is especially useful when instantaneous dose information is required for radiation protection purposes [1], monitoring radioactive contamination [2] and long term nuclear storage [3, 4] and medicine [5, 6]. Several varieties of plastic scintillating fibres are commercially available in a range of shapes, sizes, and formulations suited for different applications.

Each scintillator formulation differs mainly in light yield, fluorescence decay time, peak emission wavelength and attenuation length, all of which are provided by the manufacturer. In particular, the attenuation length, defined as the fibre length over which the intensity of the whole scintillation spectrum is reduced to 1/e, is used to describe how rapidly the scintillation light is attenuated in the fibre. In addition to standard data provided by manufacturers, attenuation lengths have been reported in a number of studies using commercial and [7, 8] and in-house fabricated plastic scintillating fibres [9]. The attenuation of guided scintillation light is a critical parameter when choosing a fibre for radiation detection as it determines the maximum practical length of the fibre and hence the overall design and operational characteristics of the sensing device. The attenuation length however, is of limited use in that it does not provide any detailed spectral information required to determine the contribution of a variety of loss sources to the total attenuation, knowledge which is critical in determining how to decrease the fibre loss, improve performance, and ultimately optimize a polymer type for a given application.

Many mechanisms contribute to light attenuation in optical fibres, and include absorption losses attributed to impurities (vis-IR), harmonics of molecular vibrations and stretching of the carbon-hydrogen bonds in the polymer (Vis-IR), electronic absorption (UV-Vis), and for polymers containing scintillating molecules, self-absorption losses (wavelengths where emission and absorption bands overlap). Light scattering from structural imperfections and defects (dust, air bubbles, scratches etc) in the fibre core also contribute to attenuation. The wavelength dependence of scattering losses by particles in the fibre core can be derived from the generalised

#345441 https://doi.org/10.1364/OME.9.000001
Journal © 2019 Received 11 Sep 2018; revised 24 Oct 2018; accepted 24 Oct 2018; published 3 Dec 2018

Optical Materials EXPRESS

Lorenz-Mie scattering theory, where the loss source can be classified as having a $1/\lambda^n$ variation. The parameter n is dependent on factors including the size, geometry, and refractive index of the scattering particle [10, 11]. The Rayleigh scattering approximation, n=4, is applicable to small spherical particles whose size is much smaller than the wavelength of light. The Mie scattering approximation applies when the particle size is comparable to the wavelength of incident light, and typically produces a wavelength dependence such that n=2, while defects larger than the wavelength results in a largely wavelength independent scattering mechanism (n=0). Another source of scattering in optical fibres is from surface capillary waves (SCWs), which are small undulations frozen in the fibre surface during fabrication and have shown to produce scattering losses which are proportional to $1/\lambda^3$ [12].

The attenuation sources described can be further categorised as intrinsic or extrinsic. Extrinsic losses include those from impurity absorption and scattering from imperfections and defects in the fibre core which are introduced during the fabrication process. Given that these losses are non-existent in an ideal fibre, they can thus be reduced by material purification and improvements to the fibre fabrication process. Among intrinsic mechanisms, there is Rayleigh scattering and absorption from electronic transitions and harmonics of the C-H bond vibrations/stretching and self-absorption losses. Intrinsic losses arise as a result of the physical and chemical structure of the fibre material, and as such cannot be eliminated, and therefore determine the ultimate fibre loss limit.

The specific wavelength dependence of each loss source makes it possible to identify and separate different attenuation effects within the fibre, and in the case of extrinsic losses, reduce or eliminate them entirely.

Here, we present the wavelength dependent attenuation for a range of commercial and in-house fabricated scintillating fibres which have been measured using a white light cut-back and side induced fluorescence (SIF) technique. The impact of scintillator formulation, fibre diameter, and cladding on the fibre loss is discussed.

2. Sources of loss in scintillating polymer optical fibres

A summary of the important loss sources in scintillating polymer fibres is presented in Table 1. Here, we will consider the effects of self-absorption, Rayleigh scattering, and defects/imperfections in the fibre core and at the core/cladding interface on fibre loss.

Table 1. Summary of sources of fibre losses

Source	Absorption losses	Scattering losses
Extrinsic	Material contaminants: -metal ions -water - organic pollutants	Defects (fractures, scratches, bubbles, dust) and imperfections (Core diameter variations) - in core - at core/clad interface
Intrinsic	C-H vibrations/stretching harmonics Electronic transitions Self-absorption	Rayleigh scattering

Rayleigh scattering is caused by density, molecular orientation and polymer composition

Optical Materials EXPRESS

fluctuations and is proportional to the fourth power of the wavelength which implies increased scattering losses at shorter wavelengths. Refractive index fluctuations caused by a broad molecular weight distribution of the polymer have shown to result in significant Rayleigh scattering losses and hence attenuation in polystyrene based optical fibre [13]. Polymers with narrow molecular weight distributions can be obtained via careful control of the polymerization process and is thus a crucial factor in fabricating a high quality polymer optical fibre. For plastic scintillators, self-absorption caused by the scintillating molecule itself, can be a significant source of intrinsic light attenuation. This effect is a result of the overlap between the materials emission and absorption bands which causes absorption of the short wavelength components of the emission spectrum, and consequently, large losses near the scintillation emission peak. This loss source is unavoidable but can be mitigated by using a scintillating dopant which has a larger wavelength difference between its excitation and absorption bands (stokes shift), by balancing the scintillating dopant concentration and limiting fibre length.

Extrinsic scattering losses arise from imperfections introduced during the fabrication process including variations in fibre geometry, bubbles/dust in the core material, and defects at the core/cladding interface. The majority of fibres used in this study have a polymer cladding layer which is formed during the fabrication process. This polymer/polymer interface confines light within the fibre core and acts as a protective coating against the surrounding environment. The outer surface of the unclad fibres (polymer/air interface) is the core itself, with the surrounding environment providing the refractive index difference necessary to confine light within the fibre core. Given the core is exposed to the environment, it is very susceptible to scattering losses via scratches and contamination on its surface. Consequently the core/clad interface, whether polymer/polymer or polymer/air will have a large impact on the fibre loss, and as such, this source of attenuation will be considered separately from other extrinsic scattering effects.

3. Techniques for loss measurements

3.1. White light cut-back technique

The cut-back method [14] was used to measure the wavelength dependent attenuation of the optical fibres between 400 and 750 nm. A 100 W halogen broadband source (approximate peak power at 800 nm) and an optical spectrum analyser (Ando AQ6315E) were used to make this measurement. Any effects on the core light coupling efficiency and subsequent power transmission caused by differences in fibre end-face quality were averaged out by carefully polishing the fibre end face flat several times to produce a new end-face at each measurement length. To ensure that only light which propagated along the whole fibre length in the core was measured, graphite based paint, DAG, was applied to the cladding at each end of the fibre, near the collection and launch points to absorb modes propagating within the PMMA (poly(methyl-methacrylate)) fibre cladding.

3.2. Side induced fluorescence (SIF) technique

An alternative method for measuring optical fibre attenuation is the SIF technique [15]. This technique is primarily used to characterise the loss mechanisms in fluorescing waveguide structures. It has the advantage of being a non-destructive procedure making it well suited for measuring losses where limited lengths of fibre are available. To perform the measurement, a 150 cm length of fibre is held straight, at a fixed vertical distance above the optical table and a monochromatic light source whose wavelength lies within the absorption band of the scintillator is used to illuminate the optical fibre from the side. Some of the resulting fluorescence produced within the core is guided by the fibre and recorded using an optical spectrum analyser (Ando AQ6315E) at its end. The fluorescence signal is maximised by adjusting the position of the diode relative to the fibre. To determine the fluorescence intensity variation as a function of fibre length, and hence the attenuation coefficient, the illumination point on the fibre is varied by translating

Optical Materials EXPRESS

the source horizontally along the fibre whilst maintaining its angle and separation relative to the fibre core.

A 365 nm UV diode (Thorlabs M365LP1, 9 nm FWHM bandwidth) was used as the excitation source, as this was a common absorption wavelength for all the scintillators characterized in this study. The fibre was kept straight to reduce bend losses and ensure the vertical illumination point on the fibre was kept constant. For the 1 mm diameter fibres fabricated in-house, the loss was determined solely using the SIF technique, as the non-destructive nature of this procedure ensured the limited lengths which were fabricated could be re-used.

4. Materials

4.1. List of materials

A list of the fibres used in this study and their relevant properties are shown in Table 2. Sample names are presented in the form X-OD(mm)a/b/c, where X represents the scintillator formulation (BCF scintillators are manufactured by Saint Gobain and EJ scintillators are manufactured by ELJEN technologies), OD is the fibre outer diameter in mm, and a, b and c are the PMMA cladding thicknesses corresponding to 0, 7.5 and 30 μm respectively. Cladding configuration d refers to a double cladding structure, where in addition to a PMMA cladding, there is an additional outer cladding layer composed of a fluor-acrylic whose refractive index (n=1.42) is lower than that of PMMA (n=1.45). The total thickness of both cladding layers in this case is 30 μm.

4.2. Commercial fibres

A range of scintillating polymer optical fibres have been sourced from a commercial supplier (Saint Gobain). All of the fibres have a circular polystyrene based core, and in some instances, a single PMMA optical cladding. Fibre B-1.5d has a double cladding configuration as explained above. The wavelength shifting fibres are formulated using an additional scintillating dopant designed to absorb the primary scintillation light and re-emit it at longer wavelengths in order to better match the sensitivity range of certain photodetectors.

4.3. In-house fabricated fibres

The in-house fibres were fabricated to achieve a wider variety of fibre diameters and scintillator formulations than the range of commercial fibres offered by Saint Gobain. Polystyrene based bulk plastic scintillators were purchased from ELJEN technologies in the form of 1 or 3 cm diameter cylindrical billets. Initial fibre fabrication trials were focused on extruding 3 cm diameter billets into rods of 1 cm diameter then drawing the rods into optical fibre. A 160 μm blue scintillator, EJ204 was fabricated using this process. The remaining two in-house fabricated fibres were drawn directly from 1 cm diameter rods acquired from the manufacturer, and include a blue (EJ204) and a green (EJ262) scintillating 1 mm diameter unclad fibre. These scintillating materials showed promise as candidates for radiation detection because of their high scintillation efficiencies, fast decay times, and reasonably long light attenuation lengths. In-house extruded and commercially supplied rods were placed in the furnace of a 4 m high drawing tower and heated to a temperature sufficiently above their glass transition temperature, T_g, which was found to be 86.4°C (measured using a PerkinElmer STA8000 simultaneous thermal analyser). Heating the polymer in excess of its T_g ensures the viscosity is lowered enough so it could be readily deformed and drawn into a fibre, which was attached to a motor driven winding drum. During fibre drawing, furnace temperature, feed speed and fibre drawing speed were adjusted to achieve a relatively stable outer diameter. Nitrogen gas was used during this process to prevent oxidation of the polystyrene.

During fabrication, the greatest stability in the outer diameter of the 160 μm fibre was attained using a furnace temperature of 350°C, a preform feed speed of 2.0 mm/min, and a draw speed

Optical Materials EXPRESS

Table 2. List of scintillator varieties used. Sample names are in the form X-OD(mm)a/b/c/d as described in Section 4.1. OD = fibre outer diameter. t_{clad} = cladding thickness. (* Double cladding structure on fibre). λ_{peak} = emission peak wavelength (Manufacturer specified). γ= scintillation efficiency for a 1 MeV electron (Manufacturer specified). ** Scintillation efficiency in PVT only as provided by manufacturer, polystyrene based materials should have a 15% reduction in efficiency. L_{att} = attenuation length, specified as the fibre length over which scintillation intensity is reduced for 1/e of initial value (Manufacturer specified). α_{bg} = background loss (dB/m) at 550 nm. λ_{edge} = wavelength (nm) at which loss is 5dB/m above α_{bg}. N/A = not applicable, listed properties apply to binary formulated scintillating materials only. N/M = not measurable, parameter outside measurable detection range.

Sample	**Scintillator**	OD (μm)	t_{clad} (μm)	λ_{peak} (nm)	γ	α_{bg} (dB/m)	λ_{edge} (nm)
A-1.0c	BCF10	1000	30	432	8000	0.92	430
B-1.0c	BCF12	1000	30	435	8000	0.69	425
B-1.0a	BCF12	1000	0	435	8000	4.12	428
B-0.25b	BCF12	250	7.5	435	8000	3.91	430
B-1.5d	BCF12	1500	30*	435	8000	0.53	425
C-1.0c	BCF20	1000	30	492	8000	0.53	490
C-1.0a	BCF20	1000	0	492	8000	3.73	492
C-0.25b	BCF20	250	7.5	492	8000	6.73	493
D-1.0c	BCF60	1000	30	530	7100	0.60	439
E-1.0c	BCF91A	1000	30	494	N/A	0.60	498
F-1.0c	BCF92	1000	30	492	N/A	0.57	491
G-1.0a	EJ204	1000	0	409	10400**	3.50	410
G-0.16a	EJ204	160	0	409	10400**	4.25	467
H-1.0a	EJ262	1000	0	481	8700**	4.25	482
I-1.0a	BCF98	1000	0	N/A	N/A	3.30	N/M

Optical Materials EXPRESS

of 9 m/min. To optimise the diameter stability of the 1 mm fibres during drawing, a furnace temperature of 355° was required with feed and draw speeds of 3 mm/min and 0.3 m/min respectively. The outer diameter of the fibres were measured during fabrication with a laser-based device and found to be 160 ± 5 μm, and 1 mm ± 25 μm.

5. Results and discussion

5.1. Predicted fibre diameters of in-house drawn fibres

Under steady state conditions, for an incompressible fluid, the relationship between the preform diameter, D_p, fibre diameter, D_f, preform feed speed v_{feed}, and the fibre drawing speed, v_{draw}, as dictated by mass conservation [16], is given by:

$$\frac{D_p^2}{D_f^2} = \frac{v_{draw}}{v_{feed}} \tag{1}$$

Although polymer is not entirely an incompressible fluid, the fibre drawing is performed at a sufficiently high temperature that the material is in the viscous regime where this equation holds true. The outer diameter of the in-house drawn fibres predicted using Eqn. (1), are compared with the measured fibre diameters in Table 3. In both cases, measured values agree well with those predicted. For fibre G-0.16a, the small deviation between the measured and predicted value can be explained by the lack of attainment of steady-state operating conditions during the fibre drawing process.

Table 3. Comparison of measured fibre diameters for in-house drawn fibres G-0.16a and H-1.0a with values predicted from Eqn. (1)

Fibre	D_p	v_{feed}	v_{draw}	$D_{calc.}$	$D_{meas.}$
G-0.16a	10 mm	2 mm/min	9 m/min	149 μm	160 ± 5 μm
H-1.0a	10 mm	3 mm/min	0.3 m/min	1000 μm	1000 ± 25 μm

5.2. Transmission losses of optical fibres

The transmission loss of each fibre in Table 2 has been measured using either the cut-back technique or the SIF technique. Where possible, both methods were used. SIF was the only measurement technique used to characterise the loss of samples B-1.5b, G-1.0b and H-1.0b. The non-destructive nature of this technique permitted re-use of the limited available lengths of G-1.0b and H-1.0b, and for sample B-1.5b, the lack of flexibility (due to the large diameter) and limited measurement space would not permit an accurate cut-back measurement. Fibre I-1.0b is an undoped polystyrene fibre, and as such, does not produce intense scintillation so the loss could only be characterised using the cut-back method. For all other samples, the attenuation values obtained using both measurement techniques are in good agreement (Fig. 1), and are within measurement error.

To represent the background loss, α_{bg}, the loss at 550 nm was selected since this wavelength does not coincide with any harmonics of the C-H vibrational/stretching or self-absorption losses. Consequently, the loss at this wavelength is largely attributed to scattering losses, both intrinsic (Rayleigh) and extrinsic (due to defects/imperfections). Additionally, the wavelength position of the attenuation edge, λ_{edge}, is listed in Table 2 for each fibre, and is taken to be the wavelength at which the loss is 5 dB/m above the background loss.

Optical Materials EXPRESS

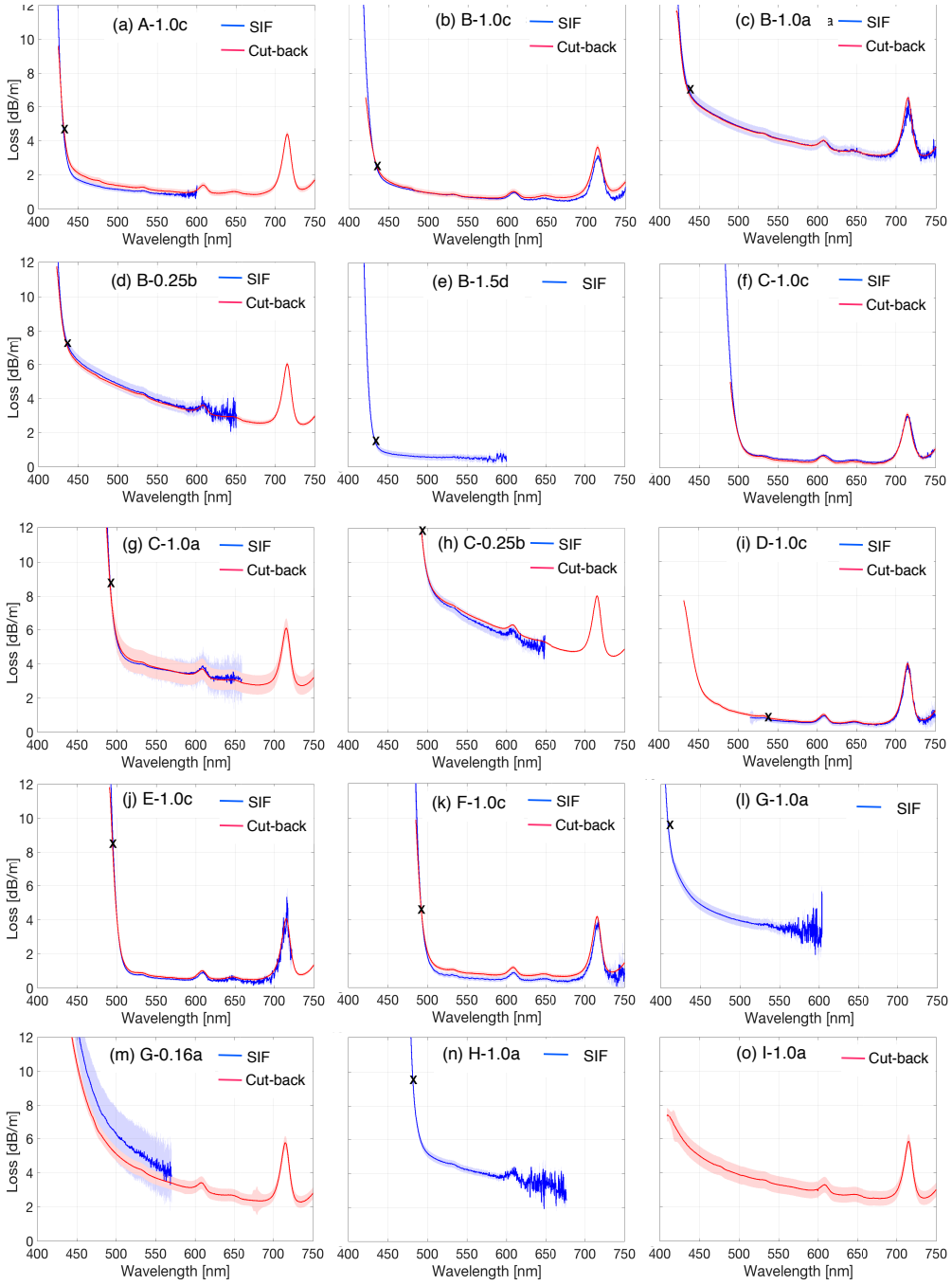

Fig. 1. Comparison of loss measurement methods for optical fibres in Table 2. The small cross represents the scintillation peak emission wavelength, provided the loss was measurable at this wavelength. The attenuation peaks at 607 and 715 nm are present in all the polystyrene based fibres tested, and are an intrinsic loss source caused by harmonics of aromatic stretching of the carbon hydrogen bonds (C-H) in the polymer [17].

Optical Materials EXPRESS

5.3. Impact of scintillator type on loss

The loss of all 1 mm PMMA cladded scintillating fibres are shown together in Fig. 2(a), and the 1 mm air cladded fibres in Figure 2(b). In each figure, the fibres differ only in their scintillator formulation, and are presented to show the effect the scintillator type has on the fibre loss without any contributing effects related to the fibre geometry. Given the core size and cladding composition are identical for the fibres in each figure, the impact of the fibre specific loss sources (core/cladding interface quality) will not be discussed.

5.3.1. Self-absorption effects

Generally, all scintillators experience a rapid increase in attenuation at wavelengths near their emission peak, λ_{peak}, largely due to the combined effects of self-absorption and Rayleigh scattering. Fibre D-1.0c does not display this characteristic attenuation edge near λ_{peak}, as it was formulated to have a larger stokes shift than the other scintillators. Specifically, the absorption band of this scintillator lies below 370 nm and the emission band begins around 480 nm, as such the self-absorption edge is located far from λ_{peak} towards the longer wavelength components of the materials absorption band. λ_{edge} (see Table 2) for all fibres is located at a similar wavelength to the emission peak with the exception of fibre D-1.0c, and as such can be a useful parameter to assess the extent of self-absorption of a particular scintillator.

At wavelengths longer than the emission peak for each scintillator (above $\approx$ 450 nm and 520 nm for blue and green scintillators, respectively), where self-absorption effects are minimal, there are three major loss contributions: wavelength dependent scattering (Rayleigh and extrinsic) and wavelength independent extrinsic scattering effects.

5.3.2. Wavelength dependent scattering losses

In figure 2(a), with the exception of D-1.0c, all fibres are shown to display the same loss slope after their emission peak (i.e wavelengths longer than λ_{edge}), hence they possess the same wavelength dependent scattering losses (Rayleigh and extrinsic). Given the high quality polymer/polymer interface of these fibres (compared to polymer/air interfaces), extrinsic scattering losses, including those with a wavelength dependence are not expected to be a major loss source, indicating scattering losses in this region are dominated by Rayleigh scattering.

The air cladded fibres in Fig. 2(b) also display similar attenuation slopes after their emission peak, and by the same argument, must possess the same wavelength dependent scattering losses. The exposure of the core to the environment in this case makes the surface susceptible to damage, so unlike the polymer cladded fibres, those with an air cladding are expected to suffer not only Rayleigh scattering in this region, but also a significant contribution from wavelength dependent scattering is expected. These scattering sources can be attributed to defects with sizes on the order of the wavelength of light (Mie scattering). Surface capillary wave scattering can also be a prominent source of loss at shorter wavelengths, and in the case of silica bandgap fibres, this surface roughness effect has been used to determine the limiting fibre loss [18]. The effects of surface capillary waves are proportional to the ratio of T_g to the surface tension of the material, γ. For silica, $T_g \approx$ 1500 K and γ= 0.3 N/m, while for polystyrene $T_g \approx$ 370 K and γ = 0.04 meaning scattering effects from these surface roughness variations are expected to be twice as high for polystyrene.

5.3.3. Wavelength independent scattering losses

At wavelengths above 520nm, Fibres A-1.0c, B-1.0c, E-1.0c and F-1.0c (Fig. 2(a)) display a higher loss offset, hence α_{bg}, relative to fibre C-1.0c. The same behavior can be observed for

Optical Materials EXPRESS

fibres B-1.0a and C-1.0a relative to G1.0a, H-1.0a and I-1.0a in Fig. 2(b). As mentioned earlier, α_{bg} is affected by extrinsic scattering losses, and to a lesser extent, Rayleigh scattering. Given the wavelength dependent scattering losses were determined to be roughly equal for either a or c type fibres, this shift in loss is attributed to higher wavelength independent scattering losses caused by larger scale defects including micron scale dust particles, bubbles, scratches and core diameter variations.

The blue scintillators generally display higher background losses, α_{bg}, at 550 nm. For a given fibre type, α_{bg} was found to vary, sometimes significantly, between different batches so the small discrepancies observed here are unlikely related to the scintillator type, and more likely a result of variations in defects introduced during polymerisation and fibre drawing.

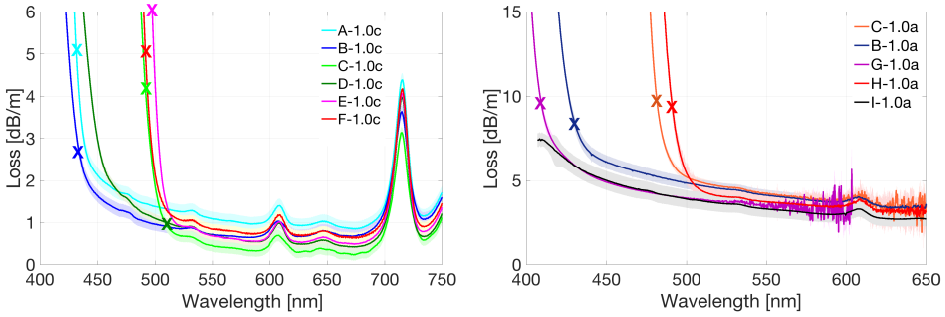

(a) (b)

Fig. 2. (a) White light loss comparison for all 1 mm cladded commercial fibres, and (b) SIF losses of in-house fabricated and commercial 1 mm air cladded scintillators and white light cutback loss of 1 mm air cladded undoped fibre. The scintillation emission peak location where applicable is marked with a small cross.

5.4. Effect of optical cladding on attenuation

The effect of fibre core diameter on attenuation is demonstrated in Figs. 3(a) and (b). For each configuration, the two scintillators differ only by the presence of a polymer cladding surrounding the core material. The polymer clad fibres display lower attenuation values over the entire wavelength range, notably, a significant decrease in α_{bg} and a reduction of the attenuation slope after the scintillator emission peak. These effects are attributed to a reduction in defects (small and large scale) at the core/clad interface, a reasonable assumption given that the cladding layer protects the core surface from contamination and defects post-fabrication. Imperfections between the polymer/polymer interface would still contribute to loss, however this effect would be minor compared to losses caused by imperfections at the polymer/air interface of air clad fibres.

5.5. Effect of core diameter on attenuation

The effect of fibre core diameter on attenuation is illustrated in Fig. 4. Both fibres in each figure below differ only in their core diameter and polymer cladding thickness (30 μm for 1.0c and 1.5d varieties vs. 7.5 μm for 0.25b varieties), however the difference in cladding thicknesses is expected to have a negligible effect on the attenuation properties of the fibre when compared with the difference in core diameter. Fibres G-1.0a and G-0.16a do not have a polymer cladding so differ only by their core diameter. As the core diameter decreases there will be a larger component of the propagating modes interacting with the core surface of the fibre, and surface scattering effects are expected to increase, consistent with the results observed here. In all cases, there is an overall increase in fibre attenuation with decreasing core diameter, which is more

Optical Materials EXPRESS

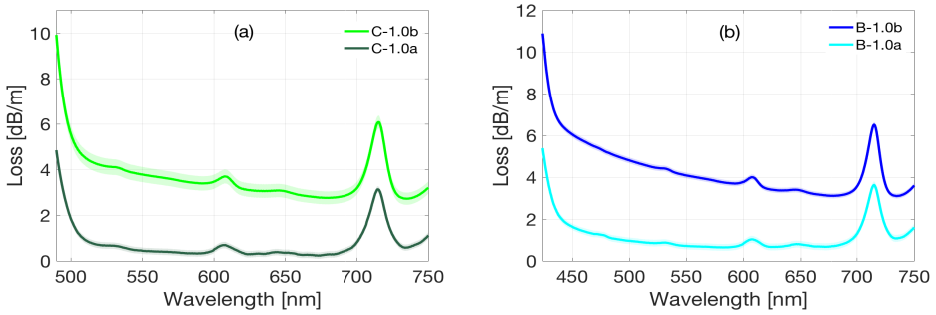

Fig. 3. Loss effects of polymer clad vs. air clad fibres

pronounced in the shorter wavelength regions where wavelength dependent surface scattering effects (Mie and SCW effects) are dominant. For fibres with a polymer/air interface, very similar background losses (Fig. 4(c)) are observed, indicating that the wavelength dependence arising from scattering by wavelength scale defects is such that they produce a loss which is negligible at 550 nm. For fibres with a polymer/polymer interface, background losses increase for smaller core fibres (Fig. 4(a) and (b)), with the most dramatic increase observed between outer diameters of 1 mm and 250 μm. In this case, the difference in background losses could be attributed to a higher degree of larger scale defects in smaller core fibres or differences in the quality of the polymer/polymer interface.

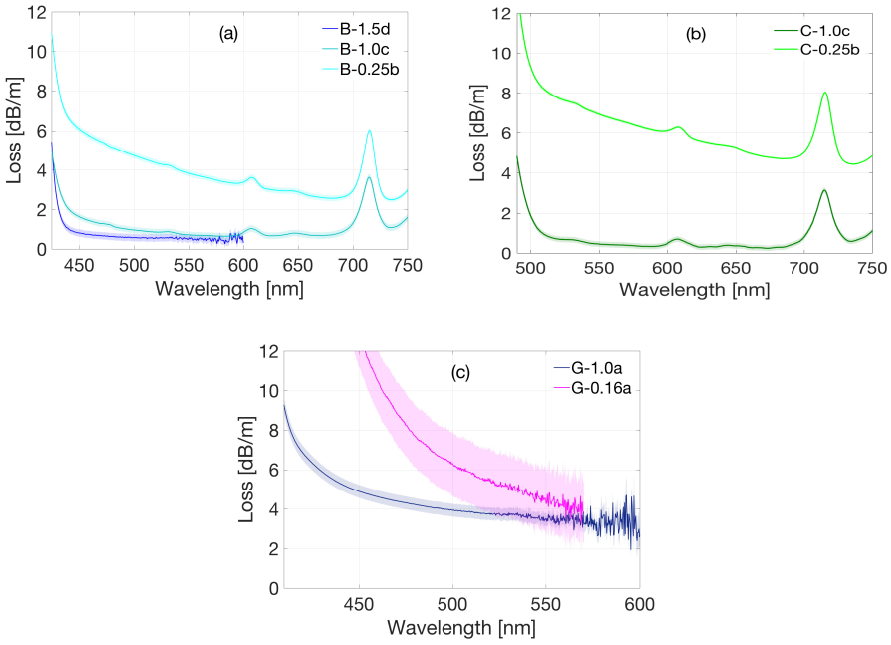

Fig. 4. Fibre core diameter effect on fibre attenuation

Optical Materials EXPRESS

6. Summary and conclusions

The wavelength dependent attenuation spectra of a range of scintillating polymer optical fibres has been measured to determine the impact of the core diameter, scintillator composition and optical cladding on the fibre loss. The major loss contribution for Polymer cladded fibres near their emission region was attributed to Rayleigh scattering, while air cladded fibres were found to display additional losses in this region attributable to wavelength dependent extrinsic scattering losses (Mie and SCW scattering) caused by small scale defects in the fibre core and core/clad interface. Small differences in the background loss were observed between fibres with the same cladding configuration, an effect caused by differences in wavelength independent scattering losses from larger (≈ micron scale) defects like scratches and contaminating particles as well as core diameter variations.

An overall increase in fibre attenuation was observed with a decrease in core diameter, an effect believed to result from the more pronounced effect of irregularities present at the core/cladding interface as the core diameter is decreased. This phenomenon can be attributed to an increased mode intensity at the core/cladding interface, hence a greater interaction with any defects on the core surface leading to increased scattering losses in the fibre as described in [16]. In this case, a reduction in the background loss, α_{bg}, by a factor of up of 12.7 was observed when the core diameter was increased from 250 μm to 1 mm (Figure 4(a) and (b)), and by a factor of 1.2 when the core diameter was increased from 160 μm to 1 mm (Fig. 4(c)). A greater improvement in α_{bg} would be expected as the core diameter is increased between 160 μm to 1 mm, however the background loss between fibres will vary depending on the optical quality of the bulk polymer which ultimately determines the limiting loss of the fibre.

Another dramatic impact on the fibre attenuation is realised when a PMMA cladding surrounds the fibre core, with polymer clad fibres displaying losses almost an order of magnitude lower than air cladded varieties. This reduction in attenuation is observed across the entire studied wavelength range for polymer cladded fibres, and is believed to result from a reduction in surface scattering losses compared to a fibre whose core is surrounded by the environment (air in this case). In general, fibres with a single PMMA cladding displayed α_{bg} values between 0.53 and 0.69 dB/m, while for air cladded fibres of the same outer diameter, α_{bg} was found to lie between 3.73 and 4.25 dB/m.

Funding

Australian Research Council Australian Copper-Uranium Transformation Research Hub (project number IH130200033).

Acknowledgments

This work was performed in part at the OptoFab node of the Australian National Fabrication Facility utilizing Commonwealth and South Australian State Government funding. This research is supported by an Australian Government Research Training Program (RTP) Scholarship. The authors acknowledge funding from the Commonwealth of Australia Defence Science and Technology Group.

Disclosures

The authors declare that there are no conflicts of interest related to this article.

References

1. A. de Andrés, Ó. Esteban, and M. Embid, "Improved extrinsic polymer optical fiber sensors for gamma-ray monitoring in radioprotection applications," Opt. & Laser Technol. **93**, 201–207 (2017).

Optical Materials EXPRESS

2. C. H. Park, J. H. Moon, and B. K. Seo, "Development of a scintillating fiber-optic sensor for the radioactive contamination measurement in a narrow area," Radiat. Meas. **46**, 687–693 (2011).
3. A. F. Fernandez, B. Brichard, S. O'Keeffe, C. Fitzpatrick, E. Lewis, J.-R. Vaille, L. Dusseau, D. Jackson, F. Ravotti, M. Glaser, and H. El-Rabii, "Real-time fibre optic radiation dosimeters for nuclear environment monitoring around thermonuclear reactors," Fusion Eng. Des. **83**, 50–59 (2008).
4. R. Kim, C. H. Park, W. J. Yoo, and J. H. Moon, "Development and characterization of a fiber-optic monitoring system for the key environment variables of the spent nuclear fuel pool at a nuclear power plant," Annals Nucl. Energy **99**, 183–192 (2017).
5. D. McCarthy, S. O'Keeffe, E. Lewis, D. Sporea, A. Sporea, I. Tiseanu, P. Woulfe, and J. Cronin, "Optical fibre radiation dosimeter for radiotherapy applications," in *2012 IEEE Sensors,* (2012), pp. 1–4.
6. A. Beddar, "Plastic scintillation dosimetry and its application to radiotherapy," Radiat. Meas. **41**, S124–S133 (2006). The 2nd Summer School on Solid State Dosimetry: Concepts and Trends in Medical Dosimetry.
7. A. Antonelli, M. Antonelli, G. Barbiellini, M. Barone, S. Bertolucci, S. Bianco, C. Bini, C. Bloise, V. Bolognesi, F. Bossi, R. Caloi, P. Campana, F. Cervelli, M. Cordelli, G. D. Zorzi, G. D. Cosimo, A. D. Domenico, O. Erriquez, F. Fabbri, A. Farilla, A. Ferrari, P. Franzini, F. Garufi, P. Gauzzi, E. Gero, S. Giovannella, R. Haydar, M. Incagli, L. Keeble, W. Kim, G. Lanfranchi, J. Lee-Franzini, A. Martini, A. Martinis, S. Miscetti, F. Murtas, A. Parri, A. Passeri, S. Sarwar, F. Scuri, E. Spiriti, L. Tortora, G. Venanzoni, X. Wang, and S. Wölfle, "Measurements of light yield, attenuation length and time response of long samples of "blue" scintillating fibers," Nucl. Instruments Methods Phys. Res. Sect. A: Accel. Spectrometers, Detect. Assoc. Equip. **370**, 367–371 (1996).
8. N. Amos, A. Bross, and M. Lundin, "Optical attenuation length measurements of scintillating fibers," Nucl. Instruments Methods Phys. Res. Sect. A: Accel. Spectrometers, Detect. Assoc. Equip. **297**, 396–403 (1990).
9. P. Rebourgeard, F. Rondeaux, J. Baton, G. Besnard, H. Blumenfeld, M. Bourdinaud, J. Calvet, J.-C. Cavan, R. Chipaux, A. Giganon, J. Heitzmann, C. Jeanney, P. Micolon, M. Neveu, T. Pedrol, D. Pierrepont, and J.-C. Thévenin, "Fabrication and measurements of plastic scintillating fibers," Nucl. Instruments Methods Phys. Res. Sect. A: Accel. Spectrometers, Detect. Assoc. Equip. **427**, 543–567 (1999).
10. P. France, *Flouride Glass Optical Fibres* (Springer Science and Business Media, 2012).
11. A. Jha, *Inorganic Glasses for Photonics: Fundamentals, Engineering, and Applications* (John Wiley & Sons, 2106).
12. H. Ebendorff-Heidepriem, S. C. Warren-Smith, and T. M. Monro, "Suspended nanowires: Fabrication, design and characterization of fibers with nanoscale cores," Opt. Express **17**, 2646–2657 (2009).
13. K. Makino, Y. Akimoto, K. Koike, A. Kondo, A. Inoue, and Y. Koike, "Low loss and high bandwidth polystyrene-based graded index polymer optical fiber," J. Light. Technol. **31**, 2407–2412 (2013).
14. J. Hect, *Understanding Fiber Optics* (Pearson Prentice Hall, 2006).
15. K. Geetha, M. Rajesh, V. P. N. Nampoori, C. P. G. Vallabhan, and P. Radhakrishnan, "Loss characterization in rhodamine 6g doped polymer film waveguide by side illumination fluorescence," J. Opt. A: Pure Appl. Opt. **6**, 4 (2004).
16. M. C. J. Large, L. Poladian, G. W. Barton, and M. A. van Eijkelenborg, *Microstructured Polymer Optical Fibres* (Springer Science & Business Media, 2008).
17. T. Kaino, "Preparation of plastic optical fibers for near-ir region transmission," J. Polym. Sci. Part A: Polym. Chem. **25**, 37–46.
18. P. J. Roberts, F. Couny, H. Sabert, B. J. Mangan, D. P. Williams, L. Farr, M. W. Mason, A. Tomlinson, T. A. Birks, J. C. Knight, and P. S. Russell, "Ultimate low loss of hollow-core photonic crystal fibres," Opt. Express **13**, 236–244 (2005).

129.127.78.216 {ts '2021-08-28 22:07:00'}